THE JOURNAL OF PHYSICAL CHEMISTRY C
A JOURNAL OF THE AMERICAN CHEMICAL SOCIETY

pubs.acs.org/JPCC

Article

Adsorption of Acrolein, Crotonaldehyde, and Cinnamaldehyde on Pt(111) Surfaces: A Comparative DFT Study

R. Ponce Perez, J. Guerrero-Sánchez, Noboru Takeuchi, and Francisco Zaera*

Cite This: J. Phys. Chem. C 2024, 128, 5532−5541

Read Online

ACCESS | Metrics & More | Article Recommendations

ABSTRACT: Using ab initio calculations, we have investigated the adsorption of both S-cis and S-trans isomers of acrolein, crotonaldehyde, and cinnamaldehyde on the Pt(111) surface at low and high surface coverages and for five types of coordinations. Emphasis was placed on identifying trends by highlighting the similarities and differences in the adsorption of all three molecules. Adsorption was found to depend on coverage: the most stable adsorption geometry at low coverages is flat, in either η^3 or η^4 coordinations with most atoms bonded to the surface, whereas a more tilted arrangement involving fewer atoms, in a η^2-C_2C_3 coordination mode, prevails at high coverages. The extra methyl group in crotonaldehyde was determined to lead to a destabilization of the multiply coordinated adsorbates at high coverages, whereas the aromatic ring in cinnamaldehyde was found to be able to bind itself to the Pt surface, at least at low coverages, and thus increase the absolute value of the adsorption energy by about 0.5 eV. Additional calculations using a noncovalent interaction index provided further insights into the variations in bonding to the surface across the three molecules versus coverage in terms of both covalent and noncovalent attractive and repulsive interactions.

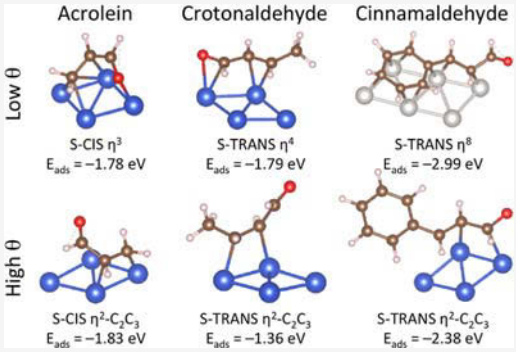

1. INTRODUCTION

Hydrogenation of organic feedstocks is at the center of many chemical industrial processes. It is commonly promoted by heterogeneous catalysts based on late transition metals such as Pt, Pd, and Rh because these metals have proved to be quite active for most hydrogenation reactions even under mild conditions. However, when reactants with multiple unsaturations are involved and specific products are sought requiring only the hydrogenation of specific bonds, platinum group catalysts have proven to display poor selectivity.[1−4] In fact, in the case of molecules with both C═C (olefinic) and C═O (carbonyl) groups, metals such as Pt tend to convert the former bonds first, a process that often leads to uninteresting products; the preferential hydrogenation of carbonyl groups in the presence of olefinic bonds, most often the desired outcome, is difficult to achieve.[5−7]

Selectivity during the catalytic hydrogenation of unsaturated aldehydes is believed to be critically dependent on the geometrical details of the way the molecules bind to the metal surface. Much research has been directed at trying to understand this correlation with particular emphasis on the details of adsorption on Pt surfaces. For instance, a combination of quantum mechanics calculations and experiments has indicated that the adsorption of acrolein on Pt(111) is strongly dependent on its coverage on the surface, with the most stable coordination being in a flat arrangement at low coverages and a more tilted geometry at high coverages.[8−12] Similar results have in general been obtained with other unsaturated aldehydes,[13] but crucial differences have also been seen due to the additional substitutions, a methyl group in crotonaldehyde[14−19] or a phenyl aromatic ring in cinnamaldehyde.[20−23] Most trends identified with pure Pt catalysts seem to hold when using Pt-containing alloys.[24,25]

In all cases, though, catalytic hydrogenation using Pt tends to yield primarily the saturated aldehyde (and/or the saturated alcohol),[26−32] a result that has been explained in terms of a preference for bonding via the C═C double bond.[33,34] With Cu-based surfaces, by contrast, adsorption via the terminal oxygen atom appears to be preferred, a geometry that favors the selective hydrogenation of the carbonyl group instead.[19,35−38] How these results vary as a function of the nature of the reactant and the conditions of the reaction has still not been fully mapped out in a systematic manner.

In this report, we provide results from density functional theory (DFT) calculations on the adsorption geometry and energy of three unsaturated aldehydes, namely, acrolein,

Received: December 12, 2023
Revised: February 5, 2024
Accepted: March 6, 2024
Published: March 20, 2024

https://doi.org/10.1021/acs.jpcc.3c08116
J. Phys. Chem. C 2024, 128, 5532−5541

crotonaldehyde, and cinnamaldehyde, in their two most characteristic isomeric forms, S-cis and S-trans, on Pt(111) surfaces, a prototypical surface with a hexagonal close-packed atomic arrangement that offers simplicity in terms of the local structure of the adsorption sites. Special focus is placed on identifying trends associated with the substitution at the terminal sp^2 carbon, from H in acrolein to CH_3 in crotonaldehyde and to C_5H_6 in cinnamaldehyde, as a function of both coverage and coordination mode to the surface. Steric effects and other noncovalent interactions (NCIs) were estimated in order to establish their participation in defining the most stable adsorption modes in each case, in particular when comparing low versus high surface coverages. It was determined that multiple coordination is in general preferred over single bonds between the oxygen atom of the unsaturated aldehyde and a Pt atom on the surface, but the final geometry was found to depend on all the parameters controlled here, namely, terminal substitution, isomeric form, coverage, and coordination mode.

2. METHODOLOGY

First-principles total energy calculations were performed to investigate the adsorption of acrolein, crotonaldehyde, and cinnamaldehyde onto the Pt(111) surface. Calculations were done using the periodic DFT as implemented in the Vienna Ab Initio Simulation Package code.[39] Electron−ion interactions were expanded using the projector-augmented wave basis[40,41] with an energy cutoff of 400 eV. Exchange−correlation energies were treated according to the Perdew−Burke−Ernzerhof parametrization in the GGA approximation,[42] and van der Waals interactions were considered employing the D3 correction method of Grimme et al.[43]

The surface was simulated by using a supercell with periodic boundary conditions and a vacuum space in the z direction larger than 20 Å to avoid interactions between adjacent slabs. The slab consisted of five atomic layers (again, in the z direction), with the two lower layers frozen in their ideal positions to simulate the bulk-like environment. Two different periodicities were considered in the $x-y$ plane with the aim of investigating the effect of the concentration of the adsorbates on their energetics and adsorption geometries: (2 × 2) and (3 × 3) supercells were used to represent high and low adsorbate coverages for acrolein and crotonaldehyde, $\theta_H = 1/4 = 0.25$ ML and $\theta_L = 1/9 = 0.11$ ML, respectively (where one monolayer, ML, is defined as one molecule per Pt surface atom), whereas larger cells, (3 × 3) and (4 × 4), were used with cinnamaldehyde to accommodate the larger molecule (Figure 1). For reference, the saturation coverages on Pt(111) for both acrolein[44] and 3-methyl-crotonaldehyde[45] have been estimated experimentally to be $\theta_{sat} \sim 0.3$ ML. As the criteria to optimize the adsorption geometries, all force components were required to be less than 0.01 eV/Å and the energy differences less than 1×10^{-4} eV. The Brillouin zone was sampled with gamma-centered k-points grids of 5 × 5 × 1 and 3 × 3 × 1 employing the Monkhorst−Pack scheme[46] for the (2 × 2) and (3 × 3) periodicities, respectively. The NCIs were calculated employing the critic2 software.[47]

3. RESULTS AND DISCUSSION

3.1. Free-Molecule Structures. For reference, the structural properties of the free molecules were calculated first, comparing the S-cis and S-trans isomers of each of the compounds considered here, namely, acrolein, crotonaldehyde, and cinnamaldehyde. The structural models of the three molecules in the two isomeric states are depicted in Figure 2, showing the atom numbering used in describing their bonding to the surface. Table 1 summarizes the bond distances calculated for the various bonds of the three molecules in their S-cis and S-trans isomeric forms, which are all consistent with the experimental values, and also the energy differences between the two isomers, to highlight that the S-trans isomer is the energetically most stable of the two, by ∼0.1 eV.

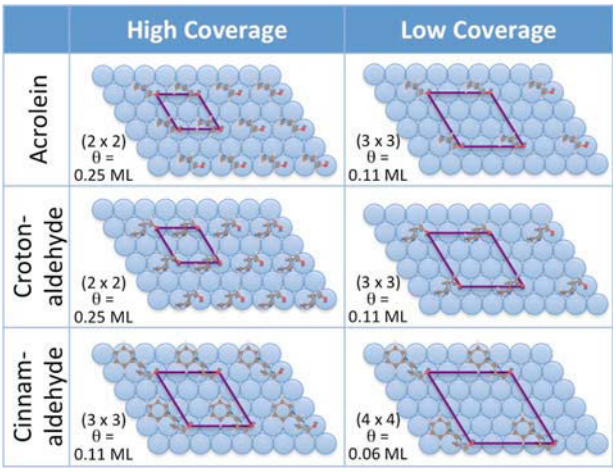

Figure 1. Surface unit cells (purple parallelograms) used to represent typical high and low surface coverages in our calculations. The molecular structures are only drawn as examples and do not indicate any optimized adsorption geometries (which are provided later).

The adsorption of acrolein and crotonaldehyde onto the Pt(111) surface was investigated next. Five different coordination modes were considered for the bonding of the molecule to the surface: (1) η^1-O, where the molecule interacts with the surface through the oxygen atom; (2,3) η^2-OC_1 and η^2-C_2C_3, where the molecule forms two bonds with the surface, either via the Pt−O and Pt−C_1 pair or involving two Pt−C bonds (Pt−C_2 and Pt−C_3), respectively, (4) η^3, where the molecule forms three bonds with the surface, and finally, (5) η^4, with all C_1, C_2, C_3, and O atom-forming bonds with the Pt surface.

3.2. Adsorption Energies. The adsorption energies (E_{ads}) of all molecules in their two isomeric forms and five possible coordination modes to the surface were estimated by using the formula

$$E_{ads} = E_{complex} - E_{suf} - E_{mol} \quad (1)$$

where $E_{complex}$ is the total energy of the system at hand and E_{surf} and E_{mol} are the total energies of the surface and the free molecule, respectively. With this definition, negative values correspond to favorable interactions, and positive values indicate that the adsorption is not favorable. The results of these calculations are summarized in Figure 3. Data are provided for the three unsaturated aldehydes studied here, namely, acrolein, crotonaldehyde, and cinnamaldehyde, adsorbed on a Pt(111) surface in both S-cis and S-trans forms and the five coordination modes mentioned above, ordered in terms of increasing degree of bonding to the surface from a η^1-O single bond to a η^4 coordination involving the oxygen atoms and the three next carbon atoms. Data are provided for both the low- and high-coverage limits.

https://doi.org/10.1021/acs.jpcc.3c08116
J. Phys. Chem. C 2024, 128, 5532−5541

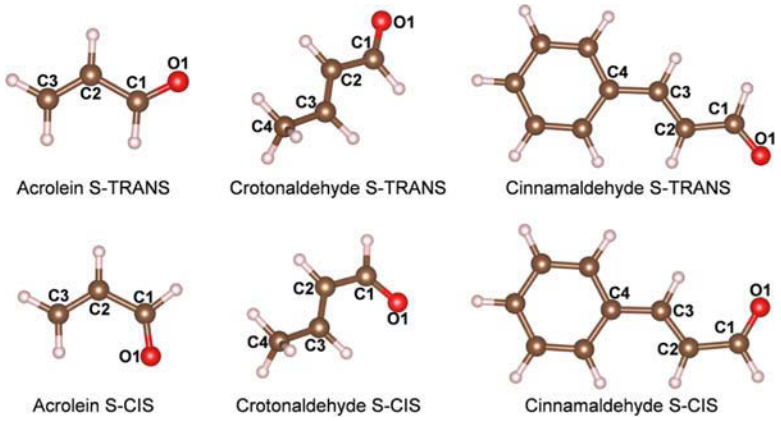

Figure 2. Structural models of the molecules studied in this work.

Table 1. Bond Distances in Acrolein, Crotonaldehyde, and Cinnamaldehyde in Their S-cis and S-trans Isomeric Forms[a]

bond	bond distance/Å					
	acrolein		crotonaldehyde		cinnamaldehyde	
	S-trans	S-cis	S-trans	S-cis	S-trans	S-cis
C_1-C_2	1.47	1.48	1.46	1.47	1.46	1.47
$C_2=C_3$	1.34	1.34	1.35	1.35	1.36	1.36
C_3-C_4			1.49	1.49	1.46	1.45
$C_1=O$	1.23	1.23	1.23	1.23	1.23	1.23
$\Delta E_{trans-cis}$/eV	−0.100		−0.095		−0.089	

[a]Also reported is the energy difference between the two isomers.

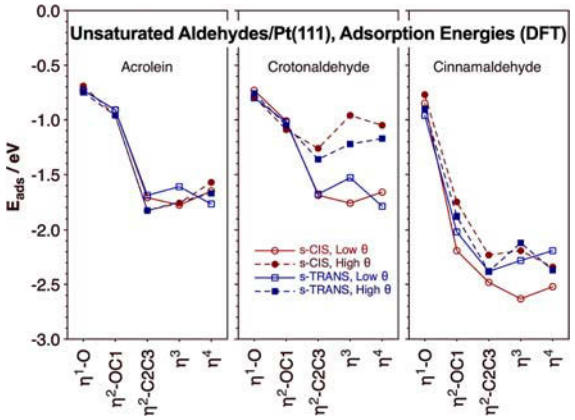

Figure 3. Calculated adsorption energies (E_{ads}) for the S-cis and S-trans isomers of acrolein (left panel), crotonaldehyde (center), and cinnamaldehyde (right) on Pt(111) at both low and high coverages.

Figure 3 highlights a number of trends associated with these adsorption energies:

1. The adsorption energy for single coordination to the surface through the oxygen atom, η^1-O, is approximately the same in all cases, that is, for both isomers of all the three molecules and at both low and high coverages: $E_{ads}(\eta^1\text{-O}) \sim 0.7$ eV. A slight increase in Pt−O bond strength can be seen with increasing substitution at the C_3 carbon, but the range of E_{ads} values only goes from a minimum of −0.69 eV for S-cis acrolein at high coverages to −0.96 eV for S-trans cinnamaldehyde at low coverages.
2. Increasing coordination to the surface results in stronger bonding in all cases. The effect is moderate when transitioning to the η^2-OC_1 coordination for acrolein and crotonaldehyde (not so for cinnamaldehyde), but larger changes are observed when considering the η^2-C_2C_3 coordination; in all cases, this binding to the surface involving the original $C_2=C_3$ bond is significantly stronger than bonding via the $C_1=O$ carbonyl moiety.
3. Additional bonding, in either a η^3 coordination involving the oxygen atom and the C_2 and C_3 carbons or a η^4 mode involving all the O, C_1, C_2, and C_3 atoms, does not add much more stability and in some cases may even result in less adsorption strength, especially at high coverages. It is likely that steric effects play a role in determining these trends, as discussed further later.
4. In the case of acrolein, neither the isomeric form nor the coverage makes much difference in its adsorption energy, but with crotonaldehyde, coverage makes a noticeable difference. It appears that the extra methyl substitution at the C_3 carbon adds a destabilizing effect.
5. At low coverages, the adsorption energies of acrolein and crotonaldehyde are fairly similar for both isomers and in all coordination cases; it is only at high coverages that the additional methyl substitution in crotonaldehyde leads to a weakening of the bonding to the surface for the high coordination cases.
6. Cinnamaldehyde shows a different behavior compared to the other two unsaturated aldehydes, with its adsorption being quite a bit stronger in all cases other than the η^1-O single coordination. In fact, much of the energy gained by multiple coordination to the surface is already reached in the η^2-OC_1 case. In addition, the phenyl aromatic ring, which is always near parallel and close to the Pt surface, provides further stability to this adsorbate.

This last point, namely, that the aromatic ring in cinnamaldehyde contributes to the stabilization of the adsorbate, was explored further. It can be seen that the C−C bonds within that ring can interact with the surface, at least at low coverages (no sufficient space is available in the high-coverage limit, namely, in the (3×3) cell, for the aromatic ring to bind flat on the surface), and rehybridize to reach an average

https://doi.org/10.1021/acs.jpcc.3c08116
J. Phys. Chem. C 2024, 128, 5532−5541

C−C bond distance of 1.46 Å. The structures of the final adsorbates for both S-cis and S-trans isomers when this consideration is added to our calculations are shown in Figure 4. The adsorption energies increase in magnitude, from −2.19 to −2.99 eV for the S-trans isomer and from −2.52 to −2.95 eV for the S-cis isomer, indicating that a Pt ring adds binding strength by an extra energy of the order of 0.4−0.8 eV.

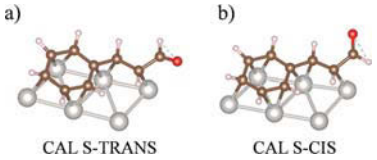

Figure 4. Cinnamaldehyde adsorption structures for the S-trans (a) and S-cis (b) isomers at low coverages obtained by including extra binding of the aromatic ring to the surface.

3.3. Adsorption Geometries. The structures calculated for the S-trans and S-cis molecules of all the three unsaturated aldehydes adsorbed onto the Pt(111) surface in their most stable configurations for each type of coordination are shown in Figures 5 and 6, respectively, and the corresponding bond distances are summarized in Table 2. These are the structures estimated using the smallest surface unit cells, which we associate with high coverages of adsorbates.

In the case of acrolein, the S-trans and S-cis isomers yield similar adsorption energy values, with η^2-C_2C_3 being the most stable coordination (E_{ads} = −1.83 eV). In those cases, the Pt−C bonds have an average distance of 2.11 Å, and the C_2═C_3 double bond rehybridizes to a single bond with a distance of 1.49 Å. The second most stable structure for the S-cis isomer of acrolein is the one with η^3 coordination, in which case both C_2═C_3 and the O═C_1 double bonds rehybridize to form single bonds; the C_2, C_3, and O atoms all interact with the surface, forming bonds with distances of 2.18, 2.08, and 2.42 Å, respectively. It is worth mentioning that the η^3 coordination for the S-trans molecule is unstable, as previously reported by Sautet et al.[9] This may be because simultaneous coordination to the surface via the C_2═C_3 double bond and the terminal oxygen atom puts much strain on the molecular skeleton after the bond rehybridization induced by bonding to the Pt atoms. The η^4 coordination is the next most stable, with E_{ads} = −1.67 and −1.57 eV for the S-trans and S-cis isomers, respectively. Here too, the double bonds of the molecule rehybridize to form single bonds, and all O, C_1, C_2, and C_3 atoms form bonds with the surface. The η^2-OC_1 and η^1 coordinations are the least stable, with adsorption energies on the order of E_{ads} ∼ −0.96 and ∼−0.70 eV, respectively.

With crotonaldehyde, η^2-C_2C_3 was found to be the most stable coordination mode as well (at high coverages), with E_{ads} = −1.36 and −1.26 eV for the S-trans and S-cis isomers, respectively. In both cases, the Pt−C bond distances are ∼2.1 Å, again indicating rehybridization to an approximately C_2−C_3 single bond. For the S-trans isomer, η^3 is the second most favorable coordination, with E_{ads} = −1.22 eV. On the other hand, for the S-cis isomer, η^2-OC_1 is the next most stable coordination instead. The third most stable coordination for both isomers is η^4, with E_{ads} = −1.17 (S-trans) and −1.05 eV (S-cis). Finally, with cinnamaldehyde once again, the η^2-C_2C_3 coordination is the most stable for the S-trans isomer, with E_{ads} = −2.38 eV, but the η^4 coordination exhibits a similar adsorption energy, E_{ads} = −2.37 eV, so both structures could coexist on the surface. For the S-cis isomer, η^4 is the most favorable bonding mode, with E_{ads} = −2.34 eV, and η^2-C_2C_3 coordination is the second most stable, with E_{ads} = −2.23 eV.

We also investigated the adsorption energies and geometries at low coverages. For this, we employed a (3 × 3) supercell for acrolein and crotonaldehyde and a (4 × 4) periodicity for cinnamaldehyde, as already indicated in the Methodology section (Figure 1). Using those unit cells, the molecules are far enough apart to reduce their interactions with each other. The structural details of the adsorbates resulting from our calculations in these cases are provided in Table 3.

In most cases, there is not much difference between the adsorption geometries of the unsaturated aldehydes in the low- versus high-coverage regimes. As indicated above, binding to the surface via the C_1═O and/or C_2═C_3 double bonds leads to their elongation due to the rehybridization induced by interaction with the metal surface. However, because in some cases the energy differences among several coordination modes are small, their stability ordering may change. These variations may be within the error of the DFT calculations, but may be worth pointing out nevertheless. For instance, the η^3 coordination is now the most favorable for the S-cis isomer of acrolein, with E_{ads} = −1.78 eV, while for the S-trans isomer,

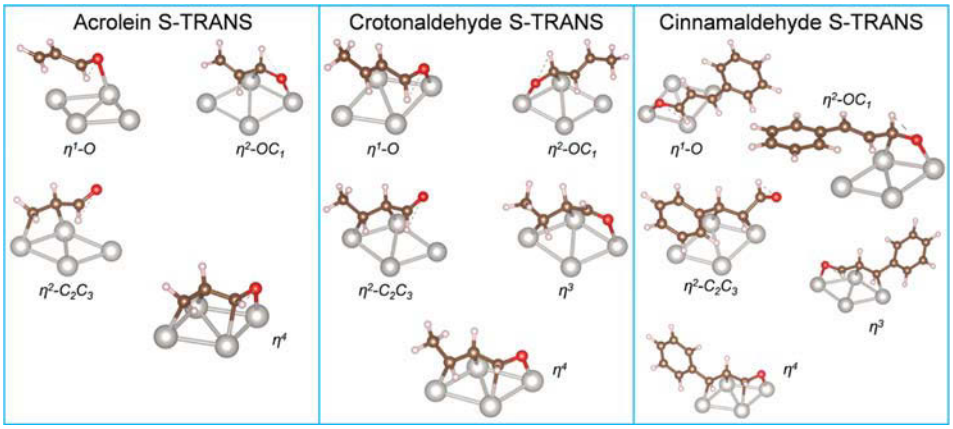

Figure 5. Calculated adsorption structures at high coverages for the S-trans isomer of the three unsaturated aldehydes studied in this project considering five different coordination modes to the surface.

https://doi.org/10.1021/acs.jpcc.3c08116
J. Phys. Chem. C 2024, 128, 5532−5541

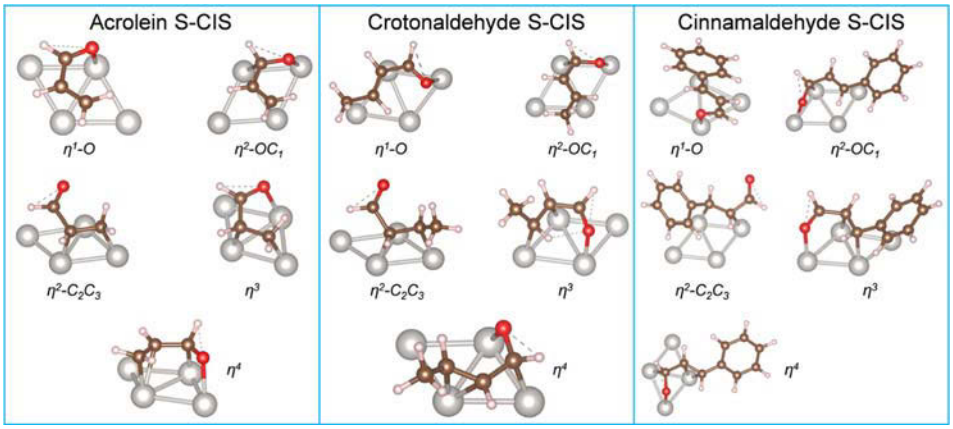

Figure 6. Calculated adsorption structures at high coverages for the S-cis isomer of the three unsaturated aldehydes studied in this project, considering five different modes of coordination to the surface.

Table 2. Bond Distance (in Å) for the Five Different Coordination Modes and the S-trans and S-cis Isomers of the Three Aldehydes Studied Here Adsorbed onto a Pt(111) Surface at High Coverages

		bond distances/Å (high coverage)					
		acrolein		crotonaldehyde		cinnamalde-hyde	
model	bond	S-trans	S-cis	S-trans	S-cis—	S-trans	S-cis
η^1-O	Pt−O	2.28	2.33	2.23	2.44	2.15	2.14
	O−C_1	1.26	1.26	1.27	1.25	1.29	1.29
	C_1−C_2	1.45	1.46	1.44	1.45	1.42	1.43
	C_2−C_3	1.35	1.35	1.35	1.35	1.37	1.37
η^2-OC_1	Pt−O	2.08	2.08	2.08	2.06	2.10	2.07
	Pt−C_1	2.15	2.15	2.16	2.16	2.17	2.17
	O−C_1	1.35	1.36	1.35	1.35	1.37	1.37
	C_1−C_2	1.48	1.48	1.47	1.47	1.46	1.45
	C_2−C_3	1.35	1.35	1.35	1.35	1.37	1.38
η^2-C_2C_3	Pt−C_2	2.14	2.15	2.11	2.09	2.13	2.14
	Pt−C_3	2.09	2.08	2.12	2.10	2.13	2.14
	O−C_1	1.22	1.24	1.22	1.22	1.26	1.26
	C_1−C_2	1.49	1.48	1.48	1.50	1.48	1.48
	C_2−C_3	1.49	1.49	1.50	1.50	1.50	1.49
η^3	Pt−O		2.42	2.48	2.11	2.18	2.17
	Pt−C_2		2.18	2.06	2.16	2.15	2.17
	Pt−C_3		2.08	2.11	2.14	2.13	2.12
	O−C_1		1.26	1.23	1.30	1.31	1.31
	C_1−C_2		1.45	1.48	1.43	1.47	1.44
	C_2−C_3		1.48	1.53	1.49	1.50	1.49
η^4	Pt−O	2.11	2.13	2.08	2.06	2.06	2.11
	Pt−C_1	2.23	2.14	2.21	2.11	2.16	2.13
	Pt−C_2	2.17	2.33	2.18	2.28	2.14	2.25
	Pt−C_3	2.09	2.14	2.14	2.28	2.13	2.21
	O−C_1	1.34	1.35	1.33	1.35	1.37	1.38
	C_1−C_2	1.48	1.47	1.48	1.47	1.50	1.48
	C_2−C_3	1.47	1.41	1.48	1.41	1.49	1.43

η^4 bonding is preferred (E_{ads} = −1.77 eV); in both cases, η^2-C_2C_3 is the second most favorable structure, with adsorption energies of $E_{ads} \sim -1.7$ eV. A similar behavior can be seen with crotonaldehyde: η^4 coordination provides the lowest energy for the S-trans isomer, E_{ads} = −1.79 eV, whereas η^3 is preferred for the S-cis counterpart (E_{ads} = −1.76 eV); η^2-C_2C_3 is again the second favorable bonding mode ($E_{ads} \sim -1.7$ eV). Nevertheless, our calculations show that in the case of acrolein, the energy difference between the most stable coordinations at high versus low coverages is approximately 50 meV, indicating that interactions among neighboring molecules do not affect the adsorption energies much. For crotonaldehyde, on the other hand, that energy difference is much larger, on the order of ∼0.5 eV, because of the steric effects mentioned above.

As already mentioned before, the case of cinnamaldehyde is unique. At low coverages, the S-cis isomer prefers the η^3 coordination (E_{ads} = −2.63 eV), even if the difference with the η^4 (E_{ads} = −2.52 eV) bonding is not too large. For the S-trans isomer, η^2-C_2C_3 is the most favorable coordination (E_{ads} = −2.38 eV), like at high coverages, but η^3 (instead of η^4) is the second most stable case (E_{ads} = −2.28 eV). It is worth noticing that for the S-trans isomer, the adsorption energies of the most stable coordination do not change much with coverage, whereas for the S-cis counterpart, a noticeable gain in binding energy to the surface can be seen at low coverages.

3.4. Noncovalent Interactions. NCIs are often critical in the interaction between molecules and surfaces and need to be included in the quantum mechanics calculations to obtain more realistic adsorption energetics. The NCI identifies the different interactions in a chemical system based on the analysis of the electron density (ρ) and its reduced gradient [$s(\rho)$],[48] with

$$s(\rho) = \frac{1}{2(3\pi^2)^{1/3}} \frac{|\rho|}{\rho^{4/3}} \quad (2)$$

On the basis of the divergent theorem, the sign of the second eigenvalue [sign(λ_2)] of the Laplacian ($\nabla^2\rho$) determines if the density at one point is concentrated or depleted and can therefore be used to distinguish between different types of interactions: bonding interactions are characterized by $\lambda_2 < 0$ (charge accumulation), whereas nonbonding interactions have $\lambda_2 > 0$ (charge depletion); van der Waals interactions show values of $\lambda_2 \sim 0$.

Here, we investigated the NCIs associated with the interaction of the three aldehydes with the Pt(111) surface. We focused on the results for low $s(\rho)$ and low ρ because that is the region where the NCIs can be identified. Figure 7 shows the dependence of $s(\rho)$ on the sign(λ_2)ρ product. The upper panels correspond to the most stable configurations at high coverages, whereas the lower panels provide the results for the low coverages, all for the η^2-C_2C_3 coordination of the S-trans

https://doi.org/10.1021/acs.jpcc.3c08116
J. Phys. Chem. C 2024, 128, 5532−5541

Table 3. Bond Distance (Å) for the Five Different Coordination Modes and Three Different Aldehydes in Their S-trans and S-cis Isomeric Forms onto the Pt(111) Surface at Low Coverages

model	bond	bond distances/Å (low coverage)					
		acrolein		crotonaldehyde		cinnamaldehyde	
		S-trans	S-cis	S-trans	S-cis	S-trans	S-cis
η^1-O	Pt−O	2.30	2.27	2.25	2.31	2.13	2.13
	O−C_1	1.26	1.26	1.26	1.26	1.29	1.29
	C_1−C_2	1.45	1.46	1.44	1.45	1.42	1.43
	C_2−C_3	1.35	1.35	1.36	1.35	1.37	1.37
η^2-OC_1	Pt−O	2.10	2.07	2.10	2.07	2.08	2.08
	Pt−C_1	2.20	2.18	2.24	2.20	2.18	2.20
	O−C_1	1.34	1.35	1.33	1.35	1.37	1.37
	C_1−C_2	1.47	1.47	1.46	1.46	1.46	1.45
	C_2−C_3	1.36	1.35	1.37	1.36	1.37	1.39
η^2-C_2C_3	Pt−C_2	2.14	2.16	2.14	2.16	2.13	2.17
	Pt−C_3	2.10	2.10	2.12	2.12	2.15	2.14
	O−C_1	1.22	1.24	1.22	1.24	1.25	1.26
	C_1−C_2	1.49	1.48	1.50	1.49	1.49	1.49
	C_2−C_3	1.49	1.49	1.50	1.49	1.50	1.49
η^3	Pt−O	2.48	2.25	2.39	2.30	2.32	2.23
	Pt−C_2	2.16	2.20	2.07	2.16	2.08	2.17
	Pt−C_3	2.10	2.08	2.12	2.11	2.14	2.13
	O−C_1	1.25	1.27	1.24	1.27	1.27	1.30
	C_1−C_2	1.48	1.45	1.49	1.46	1.49	1.45
	C_2−C_3	1.49	1.49	1.53	1.50	1.52	1.50
η^4	Pt−O	2.11	2.11	2.11	2.11	2.12	2.12
	Pt−C_1	2.22	2.19	2.19	2.18	2.11	2.35
	Pt−C_2	2.15	2.29	2.16	2.31	2.29	2.20
	Pt−C_3	2.10	2.15	1.12	2.18	2.20	2.13
	O−C_1	1.33	1.34	1.34	1.34	1.38	1.34
	C_1−C_2	1.50	1.48	1.50	1.47	1.50	1.44
	C_2−C_3	1.49	1.42	1.49	1.42	1.43	1.49
including ring binding to the surface	Pt−C_{ring}					2.20	2.20
	Pt−C_2					2.17	2.16
	Pt−C_3					2.17	2.17
	O−C_1					1.26	1.26
	C_1−C_2					1.48	1.49
	C_2−C_3					1.48	1.48

molecules. The results are shown as clusters of points, each point representing one kind of interaction in a particular region of space; since the NCI depends on the interaction distance, the electron density is modified in each region (point), and therefore, each interaction can be monitored by the modifications on the ρ and the $s(\rho)$ values. The interactions of the different moieties of the molecule with the surface have been color coded as follows: red for the CO moiety, blue for the H atom of the carbonyl group, green for the C_2 and C_3 atoms, and yellow and orange for the CH_3 group of crotonaldehyde and the aromatic ring and cinnamaldehyde, respectively. In addition, the gray color reports the interaction between the molecules.

To analyze the results, we focus on the low $\text{sign}(\lambda_2)\rho$ region between −0.1 and 0.1 and the low $s(\rho)$ range, the conditions under which the NCIs are manifested. In all cases, the carbonyl H atom experiences a mildly attractive interaction with the metal surface, as indicated by the cluster of blue dots around $\text{sign}(\lambda_2)\rho \sim -0.018$ au. On the other hand, the interaction of the CO group (red dots in Figure 7) is repulsive [$\text{sign}(\lambda_2)\rho \sim 0.012$ au]. The formation of the bonds between the C_2 and C_3 atoms and the surface, shown by the green dots, is distributed in a long range of $\text{sign}(\lambda_2)\rho$ values that extend to ∼−0.12 a.u, with an additional repulsion around the Pt−C bonds [$\text{sign}(\lambda_2)\rho \sim 0.035$ au].

In addition, with acrolein and crotonaldehyde at least, additional intermolecular interactions (gray area in Figure 7) are observed in the high-coverage regime. With acrolein, the increase in the absolute value of the adsorption energy when going from low (E_{ads} = −1.68 eV) to high (E_{ads} = −1.83 eV) coverages may be attributed to these. In the case of crotonaldehyde, by contrast, the adsorption is stronger at low coverages because of steric effects: a hydrogen bond is formed between the H atom of the methyl group of one molecule and the O atom of a neighbor, an interaction reflected in Figure 7 by the cluster of dots around $\text{sign}(\lambda_2)\rho \sim -0.025$ au. The additional dots around $\text{sign}(\lambda_2)\rho \sim 0.015$ au can be attributed to a repulsion between the C of the methyl group and an adjacent O. Additional van der Waals interactions also exist throughout the skeleton of a given molecule with its neighbors, so the methyl groups end up interacting more weakly with the surface at high coverages (yellow dots in Figure 7b versus e); this effect causes a loss in adsorption strength going from low (E_{ads} = −1.68 eV) to high (E_{ads} = −1.36 eV) coverages.

https://doi.org/10.1021/acs.jpcc.3c08116
J. Phys. Chem. C 2024, 128, 5532−5541

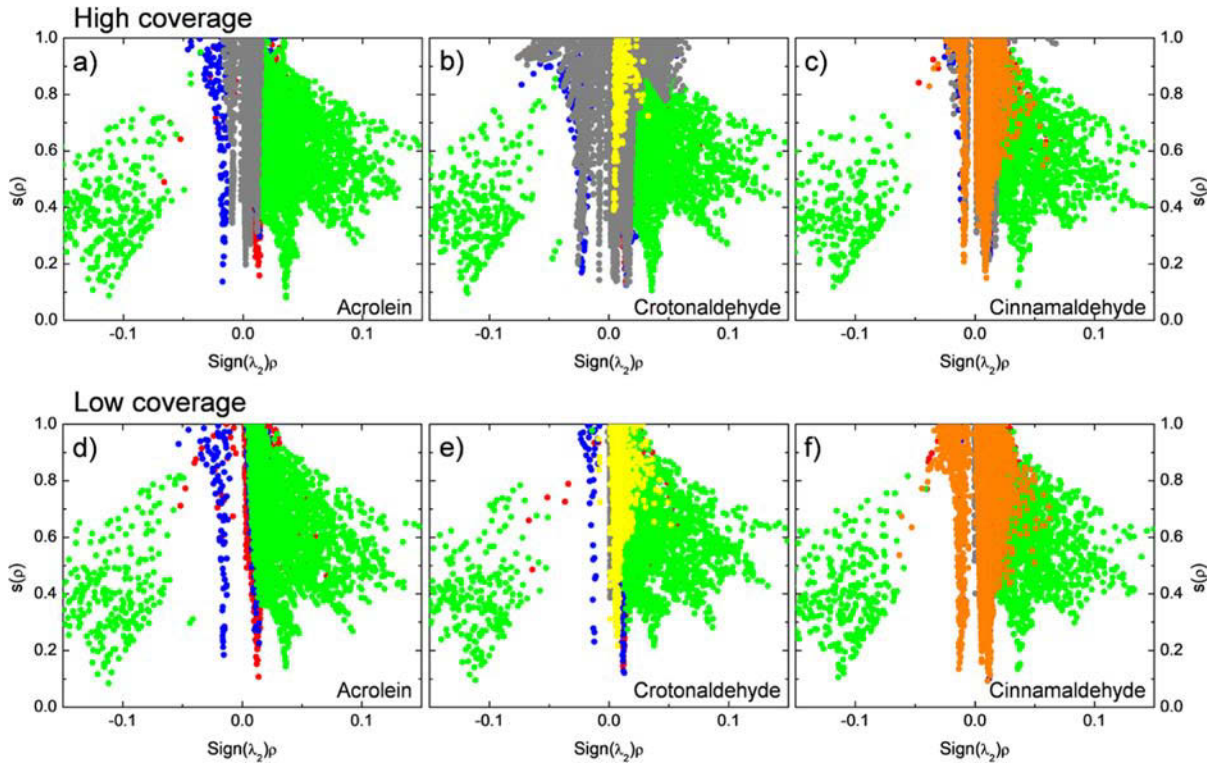

Figure 7. Reduced gradient of NCIs, $s(\rho)$, versus $\text{sign}(\lambda_2)\rho$, for the most stable configurations of the three unsaturated aldehydes at low (bottom row) and high (top) coverages. Individual interactions between specific molecular moieties and the surface are color coded, as explained in the text.

In the case of cinnamaldehyde, at high coverages (Figure 7c), the interaction between the O atom of one molecule and some of the H atoms of the aromatic ring in a neighbor is attractive, but a slight repulsion is observed between the H atoms of the ring and adjacent CO groups, leading to only some of the atoms in the aromatic ring being able to interact with the surface. At low coverages (Figure 7f), in the absence of any significant intermolecular interference, the interaction between the aromatic ring and the surface increases (orange dots). At both coverages, some of the H atoms of the aromatic ring have an attractive interaction with the neighboring molecules [$\text{sign}(\lambda_2)\rho \sim -0.01$ au], while the C attached to the C_3H_3O moiety experiences a repulsive interaction [$\text{sign}(\lambda_2)\rho \sim 0.01$ au]; the difference lies in that at low coverages the entire aromatic ring interacts (weakly, via van der Waals forces) with the surface. Because the aromatic ring always interacts with either the surface or neighboring molecules, the adsorption energies are comparable at all coverages ($E_{ads} \sim -2.38$ eV) but much larger in absolute terms compared with those of acrolein and crotonaldehyde.

The corresponding iso-surfaces for $s(\rho) = 0.5$ au for all the three molecules in their S-trans isomer form and with a η^2-C_2C_3 coordination to the surface are shown in Figure 8, for both high (left) and low (right) coverages. Attractive interactions are colored in blue, repulsive interactions in red, and van der Waals interactions in green. These images corroborate the observations discussed above. Particularly clear here are the repulsive interactions around the Pt−C bonds mentioned above. Also visible is the strong van der Waals interaction between the aromatic ring of cinnamaldehyde and the platinum surface.

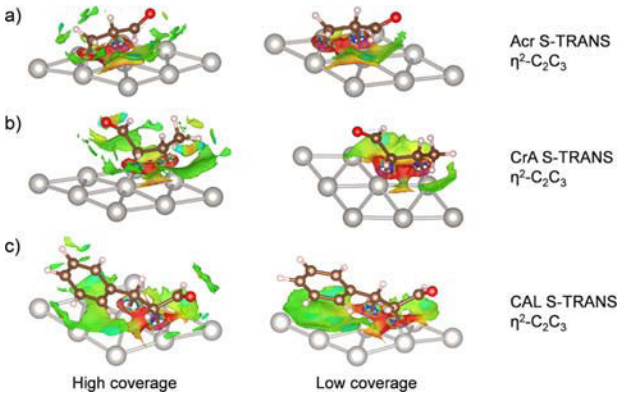

Figure 8. NCI iso-surfaces for $s(\rho) = 0.5$ au for the η^2-C_2C_3 coordination of the S-trans isomer of all the three aldehydes at both high (left column) and low (right) coverages.

The changes induced in the case of cinnamaldehyde when considering a stronger bonding of the aromatic ring to the Pt surface are highlighted for the S-trans isomer and η^2-C_2C_3 coordination in Figure 9. Figure 9a, which displays the NCI iso-surface for $s(\rho) = 0.5$ au, shows a blue region between the C atoms of the aromatic ring and the Pt atoms below that demonstrate the formation of covalent bonds between them. Notice that in this case the C_2 and C_3 atoms are also bonded to the surface, as corroborated by the blue regions around those. The $s(\rho)$ versus $\text{sign}(\lambda_2)\rho$ graph in Figure 9b supports all these conclusions: the extensive orange and green dots dispersed in a wide range of $\text{sign}(\lambda_2)\rho$ values reflect the interaction between the ring and the C_2 and C_3 atoms with the Pt surface below, respectively. The repulsive (red iso-surface) zone around the

https://doi.org/10.1021/acs.jpcc.3c08116
J. Phys. Chem. C 2024, 128, 5532−5541

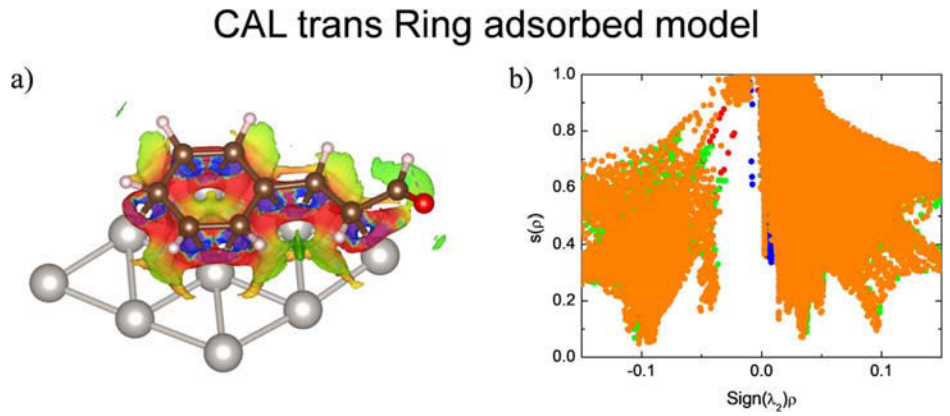

Figure 9. NCI iso-surface for $s(\rho) = 0.5$ au (a) and corresponding $s(\rho)$ versus $\text{sign}(\lambda_2)\rho$ plot (b) for S-trans cinnamaldehyde adsorbed on Pt(111) when considering the η^2-C_2C_3 coordination with additional covalent bonding of the aromatic ring to the surface.

bonds seen in Figure 9a is corroborated by the peaks at $\text{sign}(\lambda_2)\rho = 0.1$ observed in Figure 9b. It is noticed that in this configuration, the aromatic ring is the one that interacts the most with the surface, a fact that maximizes the footprint of the adsorbate. This is the reason why such configuration provides the lowest E_{ads} absolute values. Calculations with the S-cis isomer yielded similar results.

4. CONCLUSIONS

Using DFT calculations, we investigated the adsorption of acrolein, crotonaldehyde, and cinnamaldehyde onto Pt(111) surfaces at both low and high coverages. Adsorption geometries were optimized for the S-cis and S-trans isomers of each molecule in five different coordination modes with increasing number of bonds to the surface, from a single interaction via the oxygen atom to a η^4 arrangement involving the oxygen and the three carbon atoms associated with the C═O (carbonyl) and C═C moieties. Trends as different substitutions are made on the outer C═C double-bond carbon atom were identified: (1) single coordination via the oxygen atom is energetically and geometrically similar in all cases, for all aldehydes and isomers; (2) adsorption is stabilized by further coordination involving some of the carbon atoms in the molecular skeleton, but (3) the degree of stabilization with increasing coordination depends on both surface coverage and type of substitution. At high coverages, the most stable coordination in all cases was found to be a η^2-C_2C_3 bonding mode. Steric effects with neighboring molecules reduce the interaction between the surface and the molecule, preventing the latter from gaining further stability via additional coordination, as corroborated by calculations of NCI. On the other hand, at low coverage, the η^3 and η^4 coordinations do provide additional adsorption stability and thus become the prefered modes for bonding to the surface. The additional methyl substitution in going from acrolein to crotonaldehyde highlights the lowering of bonding stability induced by steric effects. On the other hand, with cinnamaldehyde, the aromatic ring can also bond to the surface and thus provide added stability, an increase of ~0.5 eV in binding energy compared to a η^4 coordination without the ring.

AUTHOR INFORMATION

Corresponding Author

Francisco Zaera − *Department of Chemistry and UCR Center for Catalysis, University of California, Riverside, California 92521, United States;* orcid.org/0000-0002-0128-7221; Email: zaera@ucr.edu

Authors

R. Ponce Perez − *Centro de Nanociencias y Nanotecnología, Universidad Nacional Autónoma de México, Ensenada, Baja California 22860, Mexico*

J. Guerrero-Sánchez − *Centro de Nanociencias y Nanotecnología, Universidad Nacional Autónoma de México, Ensenada, Baja California 22860, Mexico;* orcid.org/0000-0003-1457-9677

Noboru Takeuchi − *Centro de Nanociencias y Nanotecnología, Universidad Nacional Autónoma de México, Ensenada, Baja California 22860, Mexico*

Complete contact information is available at: https://pubs.acs.org/10.1021/acs.jpcc.3c08116

Notes

The authors declare no competing financial interest.

ACKNOWLEDGMENTS

We thank DGAPA-UNAM projects IG101124, IA100624, IN105722, and IN101523 for partial financial support. Calculations were performed in the DGTIC-UNAM Supercomputing Center under projects LANCAD-UNAM-DGTIC-51, LANCAD-UNAM-DGTIC-150, LANCAD-UNAMDGTIC-368, and LANCAD-UNAMDGTIC-422. We acknowledge the computer resources, technical expertise, and support provided by the Laboratorio Nacional de Supercómputo del Sureste de México, CONACYT member of the network of national laboratories. We thank E. Murillo and Aldo Rodriguez-Guerrero for their technical support and valuable discussions. F.Z. participation was funded by a grant from the U.S. National Science Foundation, contract no. NSF-CHE2244925.

REFERENCES

(1) Augustine, R. L. Selective Heterogeneously Catalyzed Hydrogenations. *Catal. Today* **1997**, *37*, 419−440.

(2) Blaser, H. U.; Malan, C.; Pugin, B.; Spindler, F.; Steiner, H.; Studer, M. Selective Hydrogenation for Fine Chemicals: Recent

https://doi.org/10.1021/acs.jpcc.3c08116
J. Phys. Chem. C 2024, 128, 5532−5541

Trends and New Developments. *Adv. Synth. Catal.* **2003**, *345*, 103−151.
(3) Zaera, F. The Surface Chemistry of Metal-Based Hydrogenation Catalysis. *ACS Catal.* **2017**, *7*, 4947−4967.
(4) Zhang, L.; Zhou, M.; Wang, A.; Zhang, T. Selective Hydrogenation over Supported Metal Catalysts: From Nanoparticles to Single Atoms. *Chem. Rev.* **2020**, *120*, 683−733.
(5) Gallezot, P.; Richard, D. Selective Hydrogenation of α,β-Unsaturated Aldehydes. *Catal. Rev.: Sci. Eng.* **1998**, *40*, 81−126.
(6) Luneau, M.; Lim, J. S.; Patel, D. A.; Sykes, E. C. H.; Friend, C. M.; Sautet, P. Guidelines to Achieving High Selectivity for the Hydrogenation of α,β-Unsaturated Aldehydes with Bimetallic and Dilute Alloy Catalysts: A Review. *Chem. Rev.* **2020**, *120*, 12834−12872.
(7) Lan, X.; Wang, T. Highly Selective Catalysts for the Hydrogenation of Unsaturated Aldehydes: A Review. *ACS Catal.* **2020**, *10*, 2764−2790.
(8) Loffreda, D.; Jugnet, Y.; Delbecq, F.; Bertolini, J. C.; Sautet, P. Coverage Dependent Adsorption of Acrolein on Pt(111) from a Combination of First Principle Theory and Hreels Study. *J. Phys. Chem. B* **2004**, *108*, 9085−9093.
(9) Loffreda, D.; Delbecq, F.; Sautet, P. Adsorption Thermodynamics of Acrolein on Pt (111) in Realistic Temperature and Pressure from First-Principle Calculations. *Chem. Phys. Lett.* **2005**, *405*, 434−439.
(10) Pirillo, S.; López-Corral, I.; Germán, E.; Juan, A. Density Functional Study of Acrolein Adsorption on Pt (111). *Vacuum* **2014**, *99*, 259−264.
(11) Tuokko, S.; Pihko, P. M.; Honkala, K. First Principles Calculations for Hydrogenation of Acrolein on Pd and Pt: Chemoselectivity Depends on Steric Effects on the Surface. *Angew. Chem., Int. Ed.* **2016**, *55*, 1670−1674.
(12) Fan, T.; Sun, M.; Ji, Y. First-principles study on the selective hydrogenation of the C═O and C═C bonds of acrolein on Pt−M−Pt (M = Pt, Cu, Ni, Co) surfaces. *Phys. Chem. Chem. Phys.* **2020**, *22*, 14645−14650.
(13) Haubrich, J.; Wandelt, K. Adsorption of Unsaturated and Multifunctional Molecules: Bonding and Reactivity. In *Surface and Interface Science*; Wandelt, K., Ed.; Wiley-VCH Verlag GmbH & Co. KGaA: Weinnheim, 2016; pp 529−628.
(14) de Jesús, J. C.; Zaera, F. Adsorption and Thermal Chemistry of Acrolein and Crotonaldehyde on Pt(111) Surfaces. *Surf. Sci.* **1999**, *430*, 99−115.
(15) Haubrich, J.; Loffreda, D.; Delbecq, F.; Sautet, P.; Krupski, A.; Becker, C.; Wandelt, K. Adsorption of α,β-Unsaturated Aldehydes on Pt(111) and Pt−Sn Alloys: II. Crotonaldehyde. *J. Phys. Chem. C* **2009**, *113*, 13947−13967.
(16) Cao, X.-M.; Burch, R.; Hardacre, C.; Hu, P. Reaction Mechanisms of Crotonaldehyde Hydrogenation on Pt(111): Density Functional Theory and Microkinetic Modeling. *J. Phys. Chem. C* **2011**, *115*, 19819−19827.
(17) Yang, Y.-J.; Teng, B.-T.; Liu, Y.; Wen, X.-D. Crotonaldehyde Adsorption on Ir(111), an Interesting Trans- and Cis-Configuration Transformation. *Appl. Surf. Sci.* **2015**, *357*, 369−375.
(18) Delbecq, F.; Li, Y.; Loffreda, D. Metal-Support Interaction Effects on Chemo-Regioselectivity: Hydrogenation of Crotonaldehyde on $Pt_{13}/CeO_2(111)$. *J. Catal.* **2016**, *334*, 68−78.
(19) Nayakasinghe, M. T.; Guerrero-Sánchez, J.; Takeuchi, N.; Zaera, F. Adsorption of Crotonaldehyde on Metal Surfaces: Cu Vs Pt. *J. Chem. Phys.* **2021**, *154*, 104701.
(20) Zhu, Y.; Zaera, F. Selectivity in the Catalytic Hydrogenation of Cinnamaldehyde Promoted by Pt/SiO_2 as a Function of Metal Nanoparticle Size. *Catal. Sci. Technol.* **2014**, *4*, 955−962.
(21) Durndell, L. J.; Parlett, C. M. A.; Hondow, N. S.; Isaacs, M. A.; Wilson, K.; Lee, A. F. Selectivity Control in Pt-Catalyzed Cinnamaldehyde Hydrogenation. *Sci. Rep.* **2015**, *5*, 9425.
(22) Meng, Y.; Xia, S.; Zhou, X.; Pan, G. Mechanism of Selective Hydrogenation of Cinnamaldehyde on Ni-Pt(111) with Different Structures: A Comparative Study. *Chem. Phys. Lett.* **2020**, *740*, 137049.
(23) Wang, X.; Liang, X.; Geng, P.; Li, Q. Recent Advances in Selective Hydrogenation of Cinnamaldehyde over Supported Metal-Based Catalysts. *ACS Catal.* **2020**, *10*, 2395−2412.
(24) Murillo, L. E.; Menning, C. A.; Chen, J. G. Trend in the CC and CO Bond Hydrogenation of Acrolein on Pt-M (M = Ni, Co, Cu) Bimetallic Surfaces. *J. Catal.* **2009**, *268*, 335−342.
(25) Ruvalcaba, R.; Guerrero-Sanchez, J.; Takeuchi, N.; Zaera, F. Crotonaldehyde Adsorption on Cu-Pt Surface Alloys: A Quantum Mechanics Study. *Chemistry* **2023**, *5*, 463−478.
(26) Beccat, P.; Bertolini, J. C.; Gauthier, Y.; Massardier, J.; Ruiz, P. Crotonaldehyde and Methylcrotonaldehyde Hydrogenation over Pt(111) and $Pt_{80}fe_{20}(111)$ Single Crystals. *J. Catal.* **1990**, *126*, 451−456.
(27) Ide, M. S.; Hao, B.; Neurock, M.; Davis, R. J. Mechanistic Insights on the Hydrogenation of α,β-Unsaturated Ketones and Aldehydes to Unsaturated Alcohols over Metal Catalysts. *ACS Catal.* **2012**, *2*, 671−683.
(28) Ji, X.; Niu, X.; Li, B.; Han, Q.; Yuan, F.; Zaera, F.; Zhu, Y.; Fu, H. Selective Hydrogenation of Cinnamaldehyde to Cinnamal Alcohol over Platinum/Graphene Catalysts. *ChemCatChem* **2014**, *6*, 3246−3253.
(29) Kennedy, G.; Melaet, G.; Han, H.-L.; Ralston, W. T.; Somorjai, G. A. In Situ Spectroscopic Investigation into the Active Sites for Crotonaldehyde Hydrogenation at the Pt Nanoparticle-Co_3o_4 Interface. *ACS Catal.* **2016**, *6*, 7140−7147.
(30) Yang, X.; Mueanngern, Y.; Baker, Q. A.; Baker, L. R. Crotonaldehyde hydrogenation on platinum−titanium oxide and platinum−cerium oxide catalysts: selective C═O bond hydrogen requires platinum sites beyond the oxide−metal interface. *Catal. Sci. Technol.* **2016**, *6*, 6824−6835.
(31) Dong, Y.; Zaera, F. Selectivity in Hydrogenation Catalysis with Unsaturated Aldehydes: Parallel Versus Sequential Steps. *J. Phys. Chem. Lett.* **2018**, *9*, 1301−1306.
(32) Nayakasinghe, M. T.; Xu, Y.; Zaera, F. Acrolein Hydrogenation Catalyzed by Pt(111): Effect of Carbonaceous Deposits on Kinetics. *ACS Catal.* **2023**, *13*, 14080−14089.
(33) Yang, X.; Wang, A.; Wang, X.; Zhang, T.; Han, K.; Li, J. Combined Experimental and Theoretical Investigation on the Selectivities of Ag, Au, and Pt Catalysts for Hydrogenation of Crotonaldehyde. *J. Phys. Chem. C* **2009**, *113*, 20918−20926.
(34) Haubrich, J.; Loffreda, D.; Delbecq, F.; Sautet, P.; Jugnet, Y.; Becker, C.; Wandelt, K. Adsorption and Vibrations of α,β-Unsaturated Aldehydes on Pt(111) and Pt−Sn Alloy (111) Surfaces. 3. Adsorption Energy vs Adsorption Strength. *J. Phys. Chem. C* **2010**, *114*, 1073−1084.
(35) Cao, Y.; Chen, B.; Guerrero-Sánchez, J.; Lee, I.; Zhou, X.; Takeuchi, N.; Zaera, F. Controlling Selectivity in Unsaturated Aldehyde Hydrogenation Using Single-Site Alloy Catalysts. *ACS Catal.* **2019**, *9*, 9150−9157.
(36) Chen, B.; Zaera, F. Hydrogenation of Cinnamaldehyde on Cu(110) Single-Crystal Surfaces. *J. Phys. Chem. C* **2021**, *125*, 14709−14717.
(37) Chen, B.; Ponce, R.; Guerrero-Sánchez, J.; Takeuchi, N.; Zaera, F. Cinnamaldehyde Adsorption and Thermal Decomposition on Copper Surfaces. *J. Vac. Sci. Technol., A* **2021**, *39*, 053205.
(38) Nayakasinghe, M. T.; Ponce Perez, R.; Chen, B.; Takeuchi, N.; Zaera, F. Adsorption, Thermal Conversion, and Catalytic Hydrogenation of Acrolein on Cu Surfaces. *J. Catal.* **2022**, *414*, 257−266.
(39) Kresse, G.; Furthmüller, J. Efficient Iterative Schemes for Ab Initio Total-Energy Calculations Using a Plane-Wave Basis Set. *Phys. Rev. B: Condens. Matter Mater. Phys.* **1996**, *54*, 11169−11186.
(40) Blöchl, P. E. Projector Augmented-Wave Method. *Phys. Rev. B: Condens. Matter Mater. Phys.* **1994**, *50*, 17953−17979.
(41) Kresse, G.; Joubert, D. From Ultrasoft Pseudopotentials to the Projector Augmented-Wave Method. *Phys. Rev. B: Condens. Matter Mater. Phys.* **1999**, *59*, 1758−1775.

https://doi.org/10.1021/acs.jpcc.3c08116
J. Phys. Chem. C 2024, 128, 5532−5541

(42) Perdew, J. P.; Burke, K.; Ernzerhof, M. Generalized Gradient Approximation Made Simple. *Phys. Rev. Lett.* **1996**, *77*, 3865−3868.
(43) Grimme, S.; Antony, J.; Ehrlich, S.; Krieg, H. A Consistent and Accurate Ab Initio Parametrization of Density Functional Dispersion Correction (DFT-D) for the 94 Elements H-Pu. *J. Chem. Phys.* **2010**, *132*, 154104.
(44) de Jesús, J. C.; Zaera, F. Double-Bond Activation in Unsaturated Aldehydes: Conversion of Acrolein to Propene and Ketene on Pt(111) Surfaces. *J. Mol. Catal. A: Chem.* **1999**, *138*, 237−240.
(45) Birchem, T.; Pradier, C. M.; Berthier, Y.; Cordier, G. Reactivity of 3-Methyl-Crotonaldehyde on Pt(111). *J. Catal.* **1994**, *146*, 503−510.
(46) Monkhorst, H. J.; Pack, J. D. Special Points for Brillouin-Zone Integrations. *Phys. Rev. B: Solid State* **1976**, *13*, 5188−5192.
(47) Otero-de-la-Roza, A.; Johnson, E. R.; Luaña, V. Critic2: A Program for Real-Space Analysis of Quantum Chemical Interactions in Solids. *Comput. Phys. Commun.* **2014**, *185*, 1007−1018.
(48) Johnson, E. R.; Keinan, S.; Mori-Sánchez, P.; Contreras-García, J.; Cohen, A. J.; Yang, W. Revealing Noncovalent Interactions. *J. Am. Chem. Soc.* **2010**, *132*, 6498−6506.

https://doi.org/10.1021/acs.jpcc.3c08116
J. Phys. Chem. C 2024, 128, 5532−5541